



Dynamical interaction of helium bubbles with cascade damage in Fe–9Cr ferritic alloy

Kotaro Ono^{a,*}, Mitsutaka Miyamoto^a, Kazuto Arakawa^b, R.C. Birtcher^c

^a Department of Materials Science, Shimane University, 1060 Nishi-Kawatsu, Matsue 690-8504, Japan

^b UHV-EM Center, Osaka University, Yamadaoka, Suita, Osaka 565-0871, Japan

^c MSD, Argonne National Laboratory, South Cass Avenue, Argonne, IL 60439-4838, USA

A B S T R A C T

Dynamic interaction of helium bubble with cascade damage in Fe–9Cr ferritic alloy has been studied using in situ irradiation and electron microscopy. During the irradiation of the alloy by 400 keV Fe⁺ ions at temperatures where no thermal motion takes place, induced displacement of small helium bubbles was observed: the bubbles underwent sporadic and instant displacement. The displacement was of the order of a few nanometers. The experimentally determined displacement probability of helium bubbles is consistent with the calculated probability of their dynamic interaction with sub-cascades introduced by the irradiation. Furthermore, during the irradiation of the alloy at higher temperatures, both retarded and accelerated Brownian type motions were observed. These results are discussed on the basis of dynamic interaction of helium bubbles with point defects that survive through high-energy self-ion irradiation.

© 2008 Elsevier B.V. All rights reserved.

1. Introduction

In order to develop fusion reactor materials, it is important to understand the effects of cascade damage caused by high-energy neutrons and the interaction of helium atoms with cascade damage. Therefore numerous studies have been conducted in this regard. However, limited experimental information is available on impact phenomena that occur in a cascade sequence, although many studies have been conducted on defect clusters survived cascade damage caused by irradiation with high-energy neutrons [1].

A successful technique for detecting the effects of a cascade sequence is in situ TEM observation of the dynamical response of helium bubbles to high-energy self-ion irradiation [2–4]. In the present study, we used this technique to obtain fundamental knowledge about impact effects occurring in a cascade sequence, particularly dynamic interaction of helium bubbles with cascade damage in Fe–9Cr ferritic alloy. Low activation Fe–9Cr base alloys are one of candidate structural materials, and hence it is essential to obtain information about the formation of cascade damages and its interaction with helium bubble in these alloys.

2. Experimental procedure

The material used in the present work was polycrystalline Fe–9Cr ferritic alloy that was cast from high purity starting materials.

Disk-shaped specimens of the material were pre-annealed at 1230 K for 1 h in an ultra high-vacuum furnace and then electrochemically polished for electron microscopy.

Helium bubbles were pre-introduced into the specimens by irradiation with 10 keV He⁺ ions to a fluence of about 1×10^{19} ions/m² at 820 K and then at 670 K in a JEM-2010 TEM equipped with a low energy ion accelerator. The two-step irradiation was performed in order to change the size distribution of the bubbles from a diameter of $d \sim 1.5$ nm to 4 nm. The bubble density was about 2×10^{16} /m².

In order to determine the dynamical response of helium bubbles to cascade collisions, the specimens were irradiated with 400 keV Fe⁺ ions at temperatures that ranged from room temperature to 1100 K, using an intermediate voltage electron microscope (IVEM) with a tandem ion accelerator installed at Argonne National Laboratory. The ion beam flux was about 1×10^{15} ions/m² s. Under the beam on/off conditions, the dynamical behavior of helium bubbles was continuously monitored using TEM and recorded using a video recording system. The displacements of the center position of the bubbles in the video image were measured with an error of less than 0.5 nm by using the software of Image Pro on PC.

3. Results and discussion

3.1. Depth distribution of bubbles and cascade damage

Depth distribution of helium bubbles formed by irradiation at not so high temperatures is close to a product of the damage and

* Corresponding author.

E-mail address: k-ono@riko.shimane-u.ac.jp (K. Ono).

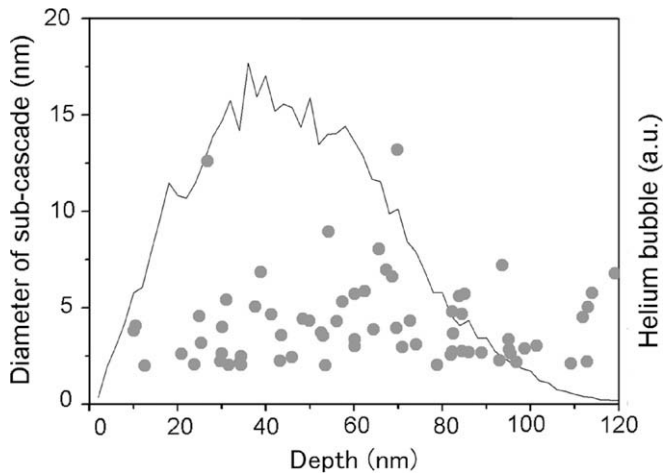


Fig. 1. Depth distributions of the diameter of sub-cascades formed by 10 ions of 400 keV Fe⁺ (●) and helium bubbles (solid line) in Fe–9Cr, calculated by TRIM code [5].

helium depositions calculated by TRIM code [5]. Fig. 1 shows thus calculated depth distribution of helium bubbles formed by irradiation with 10 keV helium ions, using a displacement-threshold energy of 23 eV. Considering the half width of this distribution, it is known that most of the bubbles are distributed in a depth range of 13–74 nm. In this figure, the size distribution of sub-cascade damage calculated by using TRIM code [5] is also plotted as a function of the depth. Here, large sub-cascades, that is, those containing more than 100 vacancies are adopted, because smaller cascades should not induce significant displacement of helium bubbles in a collision sequence. The size of a sub-cascade was estimated as the statistical standard deviation of the calculated distribution of vacancies included in the sub-cascade, assuming spherical sub-cascades. The average diameter and number of the sub-cascades per ion in the region where overlaps with the distribution of the helium bubbles in the depth from 13 nm to 74 nm, were evaluated to be 2.1 nm and 3.6, respectively.

3.2. Irradiation at low temperatures

From room temperature to about 900 K, no significant thermal motion of helium bubbles with the diameter larger than 1.5 nm took place in Fe–9Cr during the observation period of several tens of minutes [6]. However, under the irradiation of the alloy by 400 keV self-ions, sporadic displacement of helium bubbles was observed, as reported in the case of Au [3] and Cu [4]. Fig. 2(a) and (b) shows example images of helium bubbles at 0 s and 20 s, respectively, under the irradiation with 400 keV Fe⁺ ions at 770 K. The displacement of the bubbles is determined by comparing these images and is shown in Fig. 2(c), where open circles represent the bubbles shown in (a) and closed circles represent displaced ones. The average number of helium bubbles displaced during 20 s was determined from several video frames and found to be about 5%. The displacement of these bubbles was sporadic and instant, occurring in less than 0.3 s, as shown in Fig. 3, where the displacement was measured every 0.3 s. These results suggest that the displacement should be induced by the interaction of helium bubbles with effective cascade zones.

The interaction probability, M , can be given by the product of the production rate of sub-cascades and the volume of the interaction zone surrounding the cascade, as follows:

$$M = \frac{4\pi}{3} [(r_C + r_B)^3 - r_B^3] n \phi / Z, \quad (1)$$

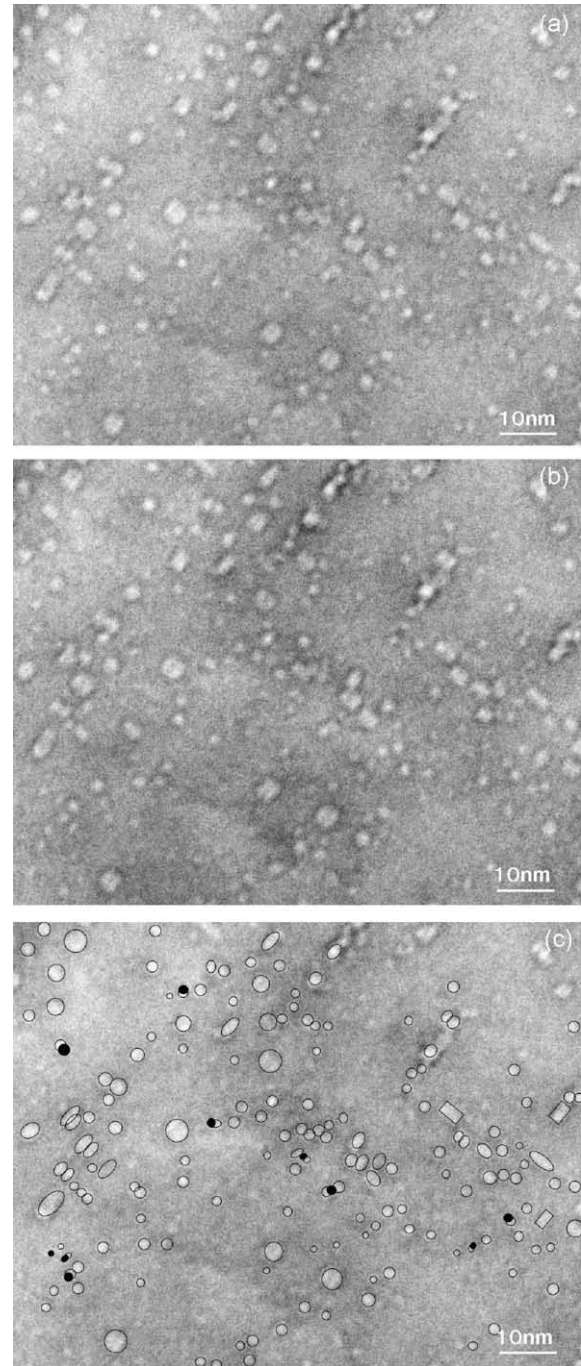


Fig. 2. Video frames of helium bubbles (a) at 0 s, (b) after irradiation of 400 keV Fe⁺ ions for 20 s, and (c) shows displacement of the bubbles from (a) (○) to (b) (●) at 770 K, where only moved ones are indicated.

where r_C and r_B denote the average radii of sub-cascades and bubbles, respectively, n denotes the number of sub-cascades per ion, ϕ the ion flux and Z the thickness of the interaction zone. From this equation, we obtain $M = 0.40\%/s$, by substituting the values $r_C = 2.1$ nm, $r_B = 1$ nm, $n = 3.2$, $\phi = 6.2 \times 10^{14}$ ions/m² s and $Z = 61$ nm, which are given by using the TRIM code [5] and the experimental conditions. On the other hand, the experimental interaction probability is $(0.25 \pm 0.1)\%/s$, which is slightly smaller than the value calculated using Eq. (1).

If the interaction of helium bubbles with a sub-cascade takes place only within a cascade zone, the interaction probability is given by

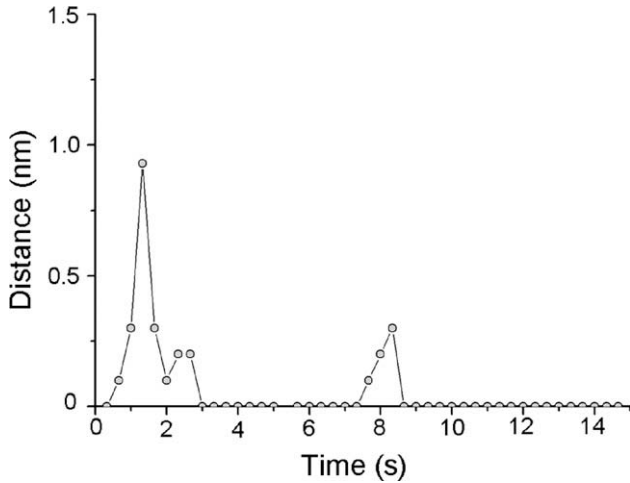


Fig. 3. Time dependence of the bubble displacement at 770 K, which was measured every 0.3 s.

$$M^* = \frac{4\pi}{3} [r_c^3] n \phi / Z. \quad (2)$$

From this equation, we obtain $M^* = 0.14\%/s$ by using the values of r_c , n , ϕ and Z mentioned above. Therefore, the experimental value of M is smaller than its theoretical value, but slightly greater than M^* . Segregated Cr on the bubble surface may reduce the displacement as reported in ref. [6], where the thermal diffusivity of helium bubbles in Fe–9Cr was reduced by segregated Cr on the bubble surface.

The present study and our previous studies on Au [3] and Cu [4] suggest that this method is useful for obtaining information about cascade effects occurring in a collision sequence. The motion of helium bubbles should be induced by thermal spike effects [7,8]. The spike temperature and high density vacancies in the sub-cascade zone could be responsible for the motion of helium bubbles.

3.3. Irradiation effects at high temperature

At high temperatures, thermal Brownian type motion of helium bubbles takes place as reported in the cases of fcc metals [9] and Fe and Fe–9Cr [6]. Fig. 4 shows the paths of representative bubbles A and B for 120 s before and during the irradiation of 400 keV Fe⁺ ions at 1085 K. In order to quantify the bubble mobility, the mean square of the migration distance $\langle R^2 \rangle$ is plotted against time t in Fig. 5, where the diffusivity D is given by $D = \langle R^2 \rangle / 4t$. As known from the figure, under the irradiation, bubble A was accelerated and Bubble B was retarded. The diffusivity of the accelerated bubble A ($d \cong 2.5$ nm) is increased from $(1.5 \pm 0.3) \times 10^{-20}$ m²/s to $(6.9 \pm 0.4) \times 10^{-20}$ m²/s, while that of the retarded bubble B ($d \cong 2.0$ nm) decreased from $(3.9 \pm 0.5) \times 10^{-20}$ m²/s to $(1.6 \pm 0.3) \times 10^{-20}$ m²/s. The number of retarded bubbles in the present experimental condition was almost same with that of accelerated ones. The retardation or acceleration of the bubble mobility should be caused by the absorption of excess vacancies or interstitial atoms that were survived from the cascade damages. By this indirect, that is, through the diffusion process of excess point defects, or even by direct interaction of helium bubbles with the cascade damage, the bubble size should be increased or decreased. The change of the bubble size critically affects the bubble mobility and the dynamical size change of helium bubbles under

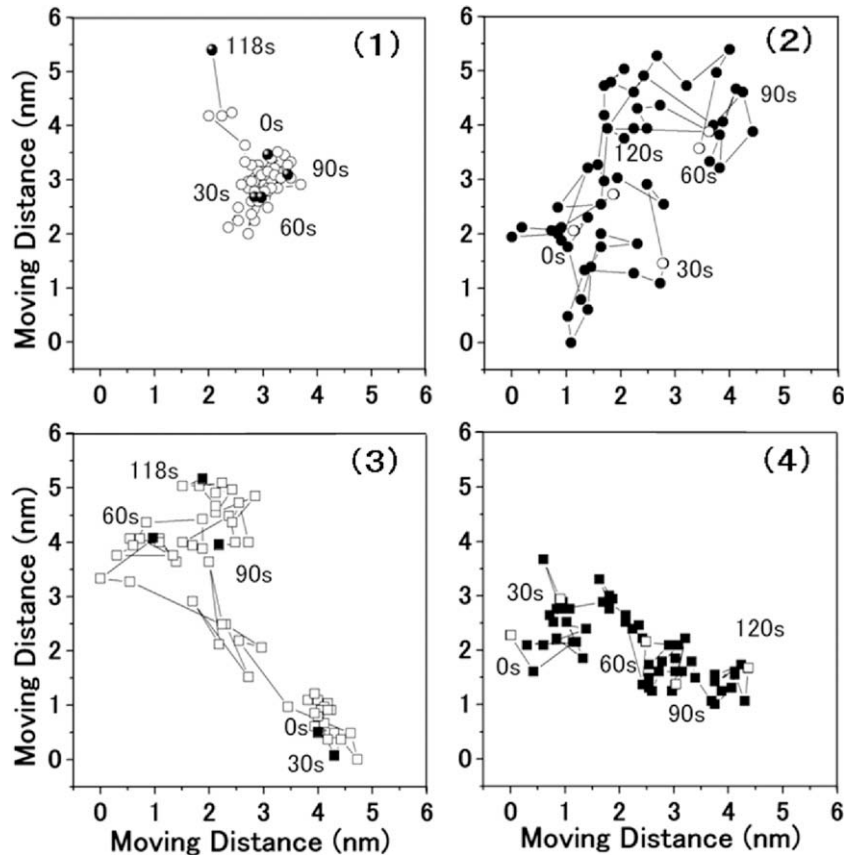


Fig. 4. Paths of the bubble migration taken every 2 s for the bubble A; (1) before the irradiation, (2) under the irradiation, and for bubble B; (3) before the irradiation, (4) under the irradiation of 400 keV Fe⁺ ions.

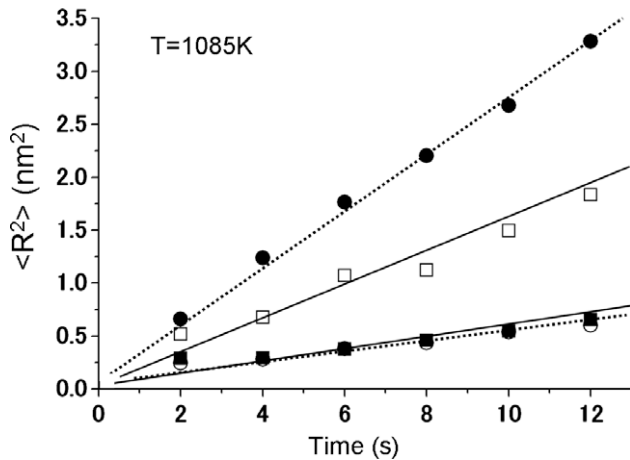


Fig. 5. Mean square of the migration distance as a function of time at 1085 K, for the bubble A: (○) before the irradiation, (●) under the irradiation, and for bubble B; (□) before the irradiation, (■) under the irradiation. The bubble A was accelerated and bubble B was retarded under the irradiation.

the high-energy self-ion irradiation was observed and the mechanism was discussed in the case of Al [10,11].

4. Summary

In this paper, dynamically responded interaction of helium bubbles with cascade damages in Fe–9Cr has been studied by in situ irradiation with 400 keV Fe⁺ ions and electron microscopy. The main results are as follows:

- (1) At low temperatures where no thermal motion takes, induced displacement of small bubbles was observed: the bubbles underwent sporadic and instant displacement. The displacement was of the order of a few nm.
- (2) The observed displacement probability of helium bubbles was about 0.25%/s and this is consistent with the probability of their interaction with sub-cascades, calculated using the TRIM code.
- (3) Both of retarded and accelerated Brownian type motions of helium bubbles were observed under the irradiation with 400 keV Fe⁺ ions at 1085 K and the mechanisms of these motions were discussed in terms of the absorption of survived vacancies or interstitial atoms from the cascade damages.

References

- [1] For example Y. Shimomura, H. Fukusima, M.W. Guinan, *J. Nucl. Mater.* 174 (1990) 210.
- [2] K. Ono, K. Arakawa, R.C. Birtcher, in: J.R. Weertman, M. Fine, K. Faber, W. King, P. Liaw (Eds.), *Electron Microscopy: Its Role in Materials Science*, TMS, 2003, p. 347.
- [3] K. Ono, M. Miyamoto, K. Arakawa, R.C. Birtcher, *Nucl. Instrum. and Meth. B* 242 (2006) 455.
- [4] M. Miyamoto, K. Ono, K. Arakawa, R.C. Birtcher, *J. Nucl. Mater.* 367–370 (2007) 350.
- [5] J.P. Biersack, L.G. Haggmark, *Nucl. Instrum. and Meth.* 174 (1980) 257.
- [6] K. Ono, K. Arakawa, K. Hojou, *J. Nucl. Mater.* 307–311 (2002) 1507.
- [7] R.S. Averback, T. Diaz de la Rubia, H. Hsieh, R. Benedek, *Nucl. Instrum. and Meth. B* 59&60 (1991) 709.
- [8] M. Ghaly, R.S. Averback, *Phys. Rev. Lett.* 72 (1994) 364.
- [9] K. Ono, K. Arakawa, K. Hojou, M. Oohashi, R.C. Birtcher, S.E. Donnelly, *J. Electron. Microsc.* 51 (2002) S245.
- [10] K. Ono, M. Miyamoto, K. Arakawa, R.C. Birtcher, *Philos. Mag.*, in press.
- [11] K. Ono, M. Miyamoto, K. Arakawa, R.C. Birtcher, *Mater. Jpn.* 45 (2006) 106.